Retrograde Melting Behavior in Polyolefin + Solvent + Antisolvent Solutions

Hertanto Adidharma and Maciej Radosz
Dept. of Chemical and Petroleum Engineering, University of Wyoming, Laramie, WY 82071

Marek Luszczyk
Institute of Physical Chemistry, Polish Academy of Sciences, 01-224 Warszawa, Poland

The SAFT1 equation of state captures the melting retrograde behavior for a ternary system of poly(ethylene-co-octene-1) + isooctane + ethylene. The melting temperature minimum depends on the polymer branch density, solvent composition, polymer concentration, and polymer molecular weight, in decreasing order of sensitivity. Furthermore, the effects of the solvent/antisolvent ratio and polymer concentration on the melting temperature are nonmonotonic, that is, their sign may change in going from low to high pressures. Finally, the sign of the slope of the melting curve depends only on the difference between the partial molar volume of polymer in solution and the molar volume of pure solid polymer.

Introduction

In order to design polymer processes, we need quantitative phase-behavior data, for example, temperature- and pressure-induced melting data usually presented as pressure–temperature (P–T) phase diagrams. Such phase diagrams illustrate the common finding that increasing pressure increases the melting temperature for pure polymers and polymer solutions. Examples of such data have been published for poly(ethylene-*co*-octene-1) in propane (Chan et al., 2000a), poly(ethylene-*co*-hexene-1) in propane, and ethylene + hexene-1 (Chan and Radosz, 2000), and polyethylene in propane (Plancher et al., 2003).

However, there is experimental evidence that the effect of pressure on the melting temperature is not always monotonic, that is, at relatively low pressures, increasing pressure can decrease the melting temperature. For example, Luszczyk and Radosz (2003) found that the crystallization and melting curves for tetracontane in propane, when plotted in P–T coordinates, exhibit a temperature minimum; the melting temperature decreases with increasing pressure at low pressures and it increases with increasing pressure at high pressure. Luszczyk and Radosz (2002) proved experimentally that tetracontane in propane can be crystallized upon decompression, which is counterintuitive, and, hence, was referred to as retrograde crystallization. We extend this term to melting as well. Such a retrograde behavior is somewhat analogous to the retrograde condensation in the critical region where a constant temperature line may cross the same phase boundary (dew point or bubble point) twice.

Similar observations have been reported for solid–liquid–vapor (SLV) systems, for example, naphthalene/CO_2, biphenyl/CO_2, vanillin/CO_2, ethyl-*o*-vanillin/CO_2, and LDPE/CO_2 (Fukné-Kokot et al., 2000), and for liquid–liquid (LL) polyalkylsiloxane blends (Imre et al., 2002).

In this work, we want to explore the extent to which a theoretically based polymer equation of state can predict such a retrograde melting in polymer solutions. We select SAFT1 (Adidharma and Radosz, 1998), because it explicitly accounts for the effects of polymer molecular weight, polymer branch density, polymer concentration, and solvent properties. We apply SAFT1 to a ternary system of poly(ethylene-*co*-octene-1) (EO) in a mixed solvent of ethylene (C2) and isooctane (iC8), for which Luszczyk and Radosz (unpublished data, 2000) took experimental data. Ethylene plays the role of an antisolvent in this system.

Correspondence concerning this article should be addressed to M. Radosz.

Calculating Solid–Liquid Transitions for EO/C2/iC8

To calculate SL transitions of polymer solutions, we need not only an equation of state, but also an approximation describing the solid state. One approximation that has been widely used for this purpose is an exclusion model described by Harismiadis and Tassios (1996), Pan and Radosz (1999), and Adidharma and Radosz (2002). In this approximation, the solid phase is pure polymer containing two discrete domains, crystalline and amorphous. Assuming that the fugacity of the crystalline part of the polymer molecule is equal to the fugacity of the polymer molecule as a whole, a thermodynamic cycle leads to the following working equation quoted from Pan and Radosz (1999)

$$\ln\left(\frac{\hat{\phi}_p^L x_p^L}{\phi_p^L}\right) = -\left[\frac{\Delta h_u}{RT_m}\left(\frac{T_m}{T}-1\right)+\frac{\Delta v P}{RT}\right]cu \qquad (1)$$

where $\hat{\phi}_p^L$ is the fugacity coefficient of polymer in solution, ϕ_p^L is the fugacity coefficient of pure liquid polymer, x_p^L is the polymer mole fraction in solution, Δh_u is the enthalpy of melting per mole crystal unit ($\approx$8220 J/mol of crystal unit), T_m is the melting temperature of pure polymer, T is the melting temperature of polymer in solution at the specified pressure P, R is the gas constant, Δv is the difference in molar volume between pure liquid and pure solid polymers at T ($\approx$4.937 cm^3/mol of crystal unit), u is the number of crystallizable units in a polymer molecule (in this case, the number of ethylene units), and c is a model parameter quantifying the fraction of the crystallizable units that are actually crystallized, which is fitted to experimental SL equilibrium data.

In order to estimate T_m, following Flory (1953), Pan and Radosz (1999) assumed that the crystal thickness is infinite. Thus, the melting point of pure copolymer is given by

$$\frac{1}{T_m} = \frac{1}{T_m^0} - \frac{R}{\Delta H_u}\ln(1-X) \qquad (2)$$

where T_m^0 is the melting temperature of pure polyethylene with infinite crystal thickness ($\approx$415 K), and X is the mole fraction of comonomer units in the copolymer. Equation 2 is a reasonable but not very accurate approximation of T_m. Its accuracy is reflected in the extent to which the exclusion model can predict the pure-polymer limit (Adidharma and Radosz, 2002).

The SAFT1 equation of state developed by Adidharma and Radosz (1998) on the basis of perturbation theory of square-well fluids (Barker–Henderson's perturbation theory) is used to calculate the fugacity coefficients. As in the work of Chan et al. (2000a), we model the EO molecules as heterosegmented chains consisting of two types of segments, the backbone type and the branch type.

The parameters for the backbone-type segments are obtained from correlations developed for long n-alkanes (Adidharma and Radosz, 1998). The parameters for the branch-type segments are assumed to have the same SAFT1 parameters as those of n-hexane, because EO has six-carbon side branches. The parameters for the two EO samples used in this work, along with those for ethylene and isooctane, are given in Table 1. We label each polymer according to its branch density (BD). Following the polymer type (EO in our case), each label specifies BD (number of branches per 100 ethyl units in the backbone) and M_n (number-averaged molecular weight). For example, EO-4-40k means EO with a BD of 4 and an M_n of 40,000.

We need five binary interaction parameters, k_{ij}, to model this ternary system, that is, $k_{\text{backbone-C2}}$, $k_{\text{branch-C2}}$, $k_{\text{backbone-iC8}}$, $k_{\text{branch-iC8}}$, and $k_{\text{C2-iC8}}$. We set $k_{\text{C2-iC8}}$ equal to zero and fit the other k_{ij} to fluid–liquid (FL) equilibrium (cloud-point) data (Luszczyk and Radosz, 2000); we do not fit any k_{ij} to the SL data. The results are shown in Table 2. Using these k_{ij}, we fit the parameter, c, needed in Eq. 1, to the melting data (Luszczyk and Radosz, 2000). As mentioned in Chan et al. (2000a), the parameter c decreases as the comonomer composition increases, as expected, but it reaches a certain limiting value at high comonomer concentration. Thus, the parameter c in this work can also be correlated as follows

$$c = 0.11808 + 0.88192\exp\left(-\frac{w_{co}}{0.95037}\right) \qquad (3)$$

Table 2. Binary Interaction Parameters k_{ij} as Empirical Functions of Temperature

	k_{ij}*	Source
C2-iC8	0	This work
Backbone-C2	$0.052652-8\times10^{-5}T$	Chan et al. (2000b)
Branch-C2	$0.01266-5\times10^{-5}T$	Chan et al. (2000b)
Backbone-iC8	$0.02427-9.56644\times10^{-5}T$	This work
Branch-iC8	-0.055	This work

*T is the temperature in K.

Table 1. SAFT1 Parameters for EO, Ethylene, and Isooctane

	m	(v^{00}) (cm^3/mol)		u^0/k (K)		λ		Source
Ethylene	1.383	14.496		146.824		1.7372		Chan et al., 2000b
Isooctane	2.966	24.292		217.975		1.7109		This work
	m†	$(v^{00})_{bb}$†	$(v^{00})_{br}$	$(u^0/k)_{bb}$†	$(u^0/k)_{br}$	$\lambda_{bb}^{\ddagger}$	λ_{br}	
EO-4-45k*	1060.449	25.202	21.086	281.903	222.578	1.6542	1.6885	This work
EO-14-76k**	1797.100	25.206	21.086	281.963	222.578	1.6542	1.6885	This work

Abbreviations: bb: backbone; *br*: branch.
*M_w = 104,300; M_n = 44,600; w_{co} = 0.139 (BD = 3.9).
**M_w = 154,000; M_n = 75,600; w_{co} = 0.387 (BD = 13.6).
†Calculated from correlations for hydrocarbons (Adidharma and Radosz, 1998).

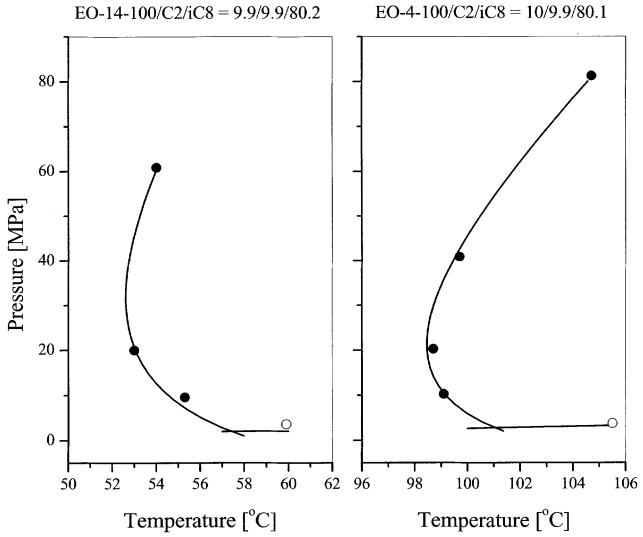

Figure 1. P–T phase diagrams for EO/C2/iC8 close to SL transitions.

Solid circles: experimental melting data; open circle: experimental VL transition; solid curves: calculated.

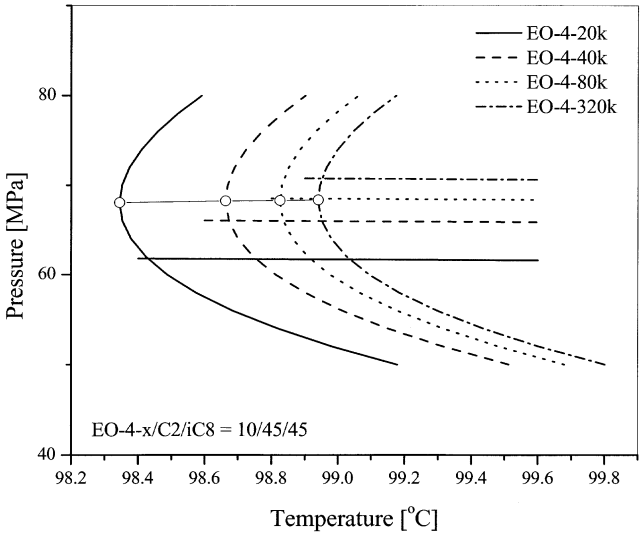

Figure 2. Effect of molecular weight on the melting temperature minimum for EO/C2/iC8.

where w_{co} is the weight fraction of comonomer (octene-1) units in the polymer.

Figure 1 shows that such a model can quantitatively represent the vapor–liquid (VL) and SL data, including the retrograde behavior, which was not part of fitting. This model is also found to represent the LL equilibria (at higher temperatures; not shown in Figure 1), which is not surprising because the LL data were used to fit k_{ij}. These LL equilibria are of the LCST-type.

Simulation Results

The purpose of the calculated SL boundaries, presented in Figures 2–6 in P–T coordinates, is to illustrate the effects of polymer molecular weight, BD, concentration, and solvent/antisolvent (iC8/C2) ratio. In these figures, the nearly horizontal lines represent FL boundaries, that is, either VL or LL boundaries. Open circles represent the SL points having the minimum melting temperatures ($T_{\min}$, P_0). We use these points to characterize the retrograde behavior. A collection of these points forms a locus shown with a light curve. The boundaries at pressures below the FL boundaries are calculated as SL transitions, and, hence, may not be a good approximation of the actual SFL boundaries; they are shown qualitatively to illustrate the slope.

Figure 2 illustrates the molecular-weight effect, which is found to be weak. For example, on going from M_n of 20 k to 320 k, $T_{\min}$ increases about 0.6°C and P_0 increases about 0.3 MPa. We also find that, when the FL boundary intersects the SL boundary above P_0, for example, for EO-4-80 k and EO-4-320 k, the melting curve does not exhibit the retrograde behavior; it monotonically increases with increasing temperature.

Figure 3 illustrates the BD effect, which is found to be stronger than that of the molecular weight: $T_{\min}$ decreases and P_0 increases with increasing BD. Also, increasing branch density is found to decrease the pressure at which the FL boundary intersects the SL boundary, which increases the probability of retrograde behavior.

Figure 4 illustrates the effect of solvent/antisolvent ratio (iC8/C2) on the retrograde behavior: $T_{\min}$ and P_0 increase with a decreasing solvent/antisolvent ratio. For example, decreasing this ratio from 8 to 1 increases $T_{\min}$ by about 2°C, and P_0 by about 45 MPa. When this ratio is low enough, for example, 1 in Figure 4, the FL boundary intersects the SL boundary above P_0, which eliminates the retrograde behavior.

Figure 4 also illustrates that, due to the retrograde behavior, changing the solvent/antisolvent ratio at constant pressure can either increase or decrease the melting temperature

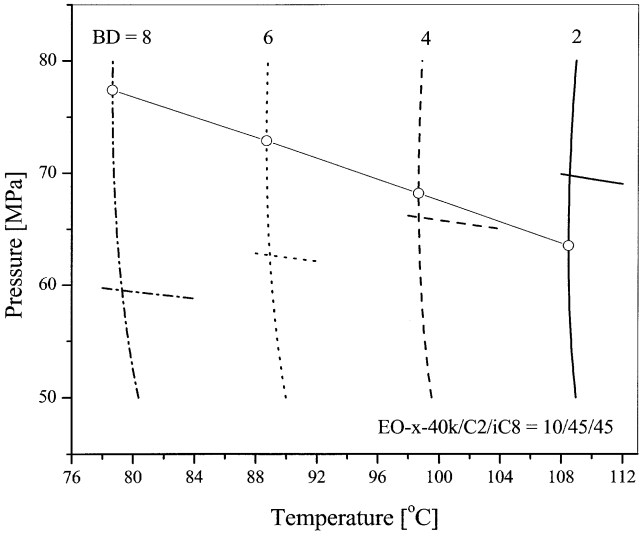

Figure 3. Effect of branch density (BD) on the melting temperature minimum for EO/C2/iC8.

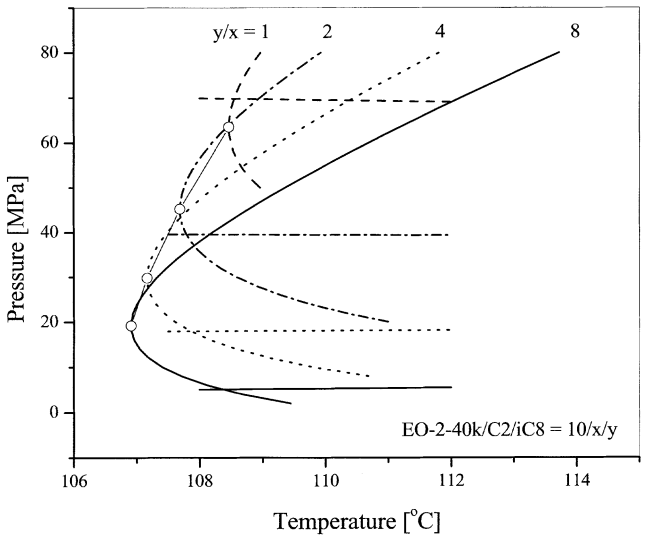

Figure 4. Effect of solvent/antisolvent ratio on the melting temperature minimum for EO/C2/iC8.

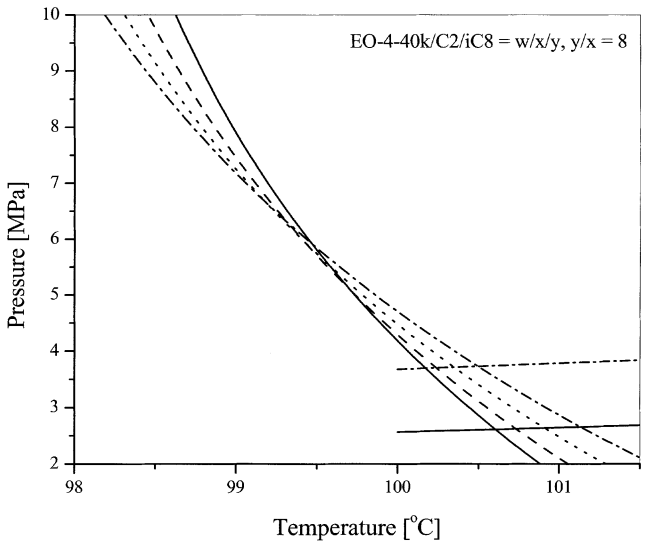

Figure 6. Effect of polymer concentration on the melting temperature minimum for EO/C2/iC8—crossover at low pressures.

depending on the pressure level. For example, at pressures higher than 30 MPa, increasing this ratio from 4 to 8 increases the melting temperature. At 22 MPa, however, increasing this ratio decreases the melting temperature.

Figure 5 illustrates the polymer concentration effect; the lower the polymer concentration the lower the T_{min} and the higher the P_0. Such a T_{min} dependence is consistent with the common experimental evidence that the polymer melting temperature generally increases with increasing concentration.

However, Figure 5 reveals an intriguing crossover at lower pressures, in the negative-slope region. This region is expanded in Figure 6. Close to the FL boundary, at constant solvent/antisolvent ratio, the melting temperature is found to decrease with increasing polymer concentration, which has never been observed experimentally.

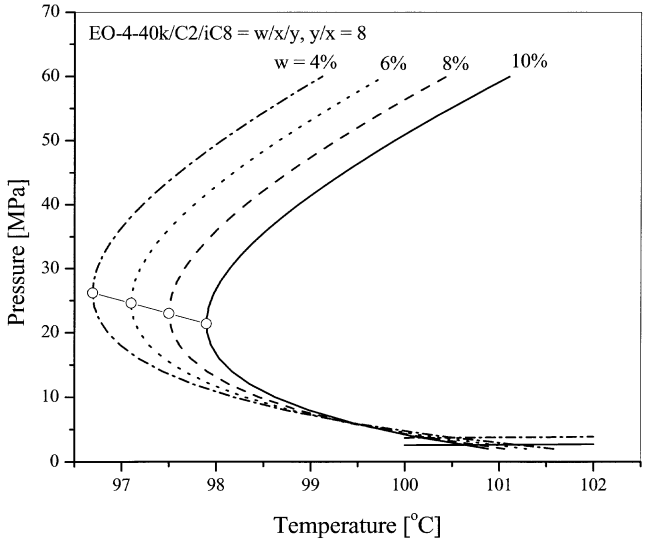

Figure 5. Effect of polymer concentration on the melting temperature minimum for EO/C2/iC8.

Thermodynamic Analysis

The nonmonotonic shape of the melting curve, with a minimum temperature, has been predicted by SAFT1 with no fitting aimed at reproducing such a retrograde behavior. We therefore use SAFT1 to analyze the equilibrium thermodynamics underlying this behavior. We start with a common assumption used in the simulation and our previous work (Chan et al., 2000a; Adidharma and Radosz, 2002), that the solid phase coexisting with the liquid phase is a pure (solvent-free) solute. It turns out that, for such an analysis, we could easily relax this assumption and come to the same conclusion.

The coexistence of solid and liquid phases requires the equality of the chemical potential for component 1 (polymer solute)

$$\mu_1^s(T,P) = \mu_1^l(T,P,x_1) \tag{4}$$

where T is the temperature, P is the pressure, μ_1^s is the chemical potential of component 1 in the solid phase, and μ_1^l is the chemical potential of component 1 in the liquid phase. The chemical potential of a solute in the solid phase is independent of composition, as we assume that the solid phase is pure solute.

For differential changes around the state of equilibrium, Eq. 4 becomes

$$d\mu_1^s(T,P) = d\mu_1^l(T,P,x_1) \tag{5}$$

Thus

$$\frac{\partial \mu_1^s}{\partial T}dT + \frac{\partial \mu_1^s}{\partial P}dP = \frac{\partial \mu_1^l}{\partial T}dT + \frac{\partial \mu_1^l}{\partial P}dP + \frac{\partial \mu_1^l}{\partial x_1}dx_1 \tag{6}$$

At constant composition, substituting the identities

$$\left(\frac{\partial \mu_1}{\partial T}\right)_P = -\bar{s}_1 \tag{7}$$

$$\left(\frac{\partial \mu_1}{\partial P}\right)_T = \bar{v}_1 \tag{8}$$

where $\bar{s}_1$ is the partial molar entropy of component 1 and $\bar{v}_1$ is the partial molar volume of component 1, yields

$$\left(\bar{s}_1^l - s_1^s\right)dT = \left(\bar{v}_1^l - v_1^s\right)dP \tag{9}$$

where s_1^s is the molar entropy of pure solid 1 and v_1^s is the molar volume of pure solid 1.

Equation 4 can also be expanded to obtain

$$\left(\bar{s}_1^l - s_1^s\right) = \frac{\left(\bar{h}_1^l - h_1^s\right)}{T} \tag{10}$$

where $\bar{h}_1^l$ is the partial molar enthalpy of component 1 in the liquid phase and h_1^s is the molar enthalpy of pure solid 1. Substituting this relation into Eq. 9 yields

$$\frac{dP}{dT} = \frac{\left(\bar{h}_1^l - h_1^s\right)}{T\left(\bar{v}_1^l - v_1^s\right)} \tag{11}$$

or

$$\frac{dP}{dT} = \frac{1}{T}\frac{\left(\bar{h}_1^l - h_1^l\right) + \Delta h_1}{\left(\bar{v}_1^l - v_1^s\right)} \tag{12}$$

where h_1^l is the molar enthalpy of pure liquid 1 and Δh_1 is the molar enthalpy of melting of pure solid 1 given by

$$\Delta h_1 = h_1^l - h_1^s \tag{13}$$

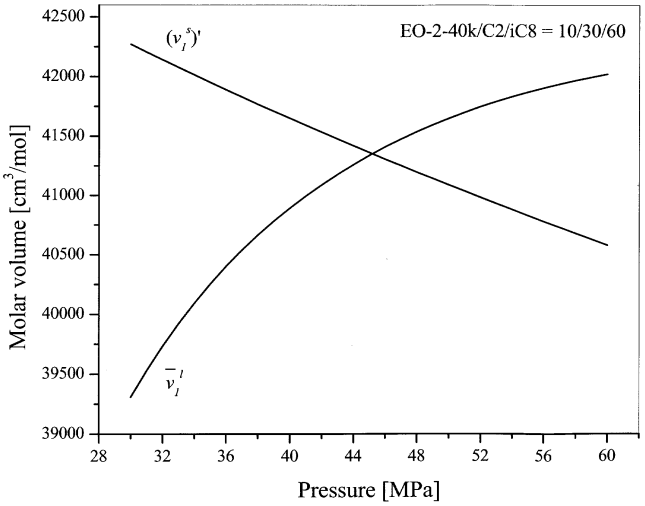

Figure 7. Molar values, $\bar{v}_1^l$ and $(v_1^s)'$, for EO-2-40k/C2/iC8 along the melting curve predicted using SAFT1.

Since $\Delta h_1 \gg |\bar{h}_1^l - h_1^l|$, and is positive, the sign of the slope of the melting curve, that is, Eq. 12, depends on its denominator, that is, the volume terms. When $\bar{v}_1^l > v_1^s$, dP/dT is positive, and, thus, the melting temperature increases with increasing pressure. Conversely, when $\bar{v}_1^l < v_1^s$, dP/dT is negative, and the melting temperature decreases with increasing pressure.

To apply this analysis quantitatively to our model, we need to differentiate Eq. 1 instead of using Eq. 12 directly, because an assumption that Δv is constant ($\approx$4.937 cm^3/mol crystal unit) has been made in developing the model. By differentiating Eq. 1, the denominator of dP/dT becomes

$$\bar{v}_1^l - \left(v_1^s\right)' \tag{14}$$

where $(v_1^s)'$ is the predicted molar volume of pure solid 1 given by

$$\left(v_1^s\right)' = v_1^l - cu\Delta v \tag{15}$$

The partial molar volume of component 1 in the liquid phase can be calculated using

$$\bar{v}_1^l = RT\left(\frac{\partial \ln\left(\hat{f}_1^l\right)}{\partial P}\right)_{T,x} \tag{16}$$

where $\hat{f}_1^l$ is the fugacity of component 1 in the liquid phase.

Figure 7 shows the values of $\bar{v}_1^l$ and $(v_1^s)'$ for EO-2-40k/ethylene/isooctane along the melting curve predicted using SAFT1. When $\bar{v}_1^l > (v_1^s)'$, dP/dT is positive, and, thus, the melting temperature increases with increasing pressure. Conversely, when $\bar{v}_1^l < (v_1^s)'$, dP/dT is negative and the melting temperature decreases with increasing pressure. At $P \approx 45$ MPa, $\bar{v}_1^l = (v_1^s)'$ and the melting temperature reaches its minimum, which is consistent with the curve for the solvent/antisolvent ratio of 2 in Figure 4.

Conclusion

The SAFT1 equation of state is found to capture the melting retrograde behavior (a temperature minimum on the PT melting curve) for a ternary system of EO/C2/iC8. The calculated melting temperature minimum is found to depend on the following system conditions: polymer branch density, solvent/antisolvent ratio, polymer concentration, and polymer molecular weight, in decreasing order of sensitivity. Furthermore, the effects of the solvent/antisolvent ratio and polymer concentration on the melting temperature are found to be nonmonotonic, that is, their sign may change in going from low to high pressures. Finally, the sign of the slope of the melting curve is found to depend only on the difference between the partial molar volume of polymer in solution and the molar volume of pure solid polymer.

Acknowledgment

This work was supported by NSF Grant CTS-9908610.

Literature Cited

Adidharma, H., and M. Radosz, "Prototype of an Engineering Equation of State for Heterosegmented Polymers," *Ind. Eng. Chem. Res.*, **37**, 4453 (1998).

Adidharma, H., and M. Radosz, "Inclusion and Exclusion Approximations of Copolymer Solids Applied to Calculation of Solid-Liquid Transitions," *Ind. Eng. Chem. Res.*, **41**, 1774 (2002).
Chan, K. C., H. Adidharma, and M. Radosz, "Fluid-Liquid and Fluid-Solid Transitions of Poly(ethylene-*co*-octene-1) in Sub- and Supercritical Propane Solutions," *Ind. Eng. Chem. Res.*, **39**, 3069 (2000a).
Chan, K. C., H. Adidharma, and M. Radosz, "Fluid-Liquid Transitions of Poly(ethylene-co-octene-1) in Supercritical Ethylene Solutions," *Ind. Eng. Chem. Res.*, **39**, 4370 (2000b).
Chan, K. C., and M. Radosz, "Fluid-Liquid and Fluid-Solid Phase Behavior of Poly(ethylene-co-hexene-1) Solutions in Sub- and Supercritical Propane, Ethylene, and Ethylene + Hexene-1," *Macromolecules*, **33**, 6800 (2000).
Flory, P. J., *Principles of Polymer Chemistry*, Cornell Univ. Press, Ithaca, NY (1953).
Fukné-Kokot, K., A. König, Z. Knez, and M. Skerget, "Comparison of Different Methods for Determination of the S-L-G Equilibrium Curve of a Solid Component in the Presence of a Compressed Gas," *Fluid Phase Equilib.*, **173**, 297 (2000).
Harismiadis, V. I., and D. P. Tassios, "Solid-Liquid-Liquid Equilibria in Polymer Solutions," *Ind. Eng. Chem. Res.*, **35**, 4667 (1996).
Imre, A. R., T. Kraska, and L. Yelash, "The Effect of Pressure on the Liquid-Liquid Phase Equilibrium of Two Polydisperse Polyalkylsiloxane Blends," *Phys. Chem. Chem. Phys.*, **4**, 992 (2002).
Luszczyk, M., and M. Radosz, "Temperature- and Pressure-Induced Crystallization and Melting of Tetracontane in Propane," *J. Chem. Eng. Data*, in press (2003).
Pan, C., and M. Radosz, "Modeling of Solid-Liquid Equilibria in Naphthalene, Normal-Alkane and Polyethylene Solutions," *Fluid Phase Equilib.*, **155**, 57 (1999).
Plancher, H., H. Adidharma, and M. Radosz, "Rate and Heat-Treatment Effects on Crystallization, Melting, and Fluid-Liquid Transitions in Dilute Polyethylene Solutions in Propane," *Ind. Eng. Chem. Res.,* in press (2003).

Manuscript received May 28, 2002, and revision received Sept. 13, 2002.